



HAL
open science

On the Petri Nets Control of the Multicellular Converter

Philippe Djondiné, Jean-Pierre Barbot, Malek Ghanes

► **To cite this version:**

Philippe Djondiné, Jean-Pierre Barbot, Malek Ghanes. On the Petri Nets Control of the Multicellular Converter. International Journal of Emerging Technology and Advanced Engineering, 2017, 7 (11), pp.332-336. hal-01896760

HAL Id: hal-01896760

<https://hal.science/hal-01896760>

Submitted on 18 Oct 2018

HAL is a multi-disciplinary open access archive for the deposit and dissemination of scientific research documents, whether they are published or not. The documents may come from teaching and research institutions in France or abroad, or from public or private research centers.

L'archive ouverte pluridisciplinaire **HAL**, est destinée au dépôt et à la diffusion de documents scientifiques de niveau recherche, publiés ou non, émanant des établissements d'enseignement et de recherche français ou étrangers, des laboratoires publics ou privés.

On the Petri Nets Control of the Multicellular Converter

Philippe Djondiné¹, Jean-Pierre Barbot², Malek Ghanes³

¹*Department of Physics, Faculty of Science, The University of Ngaoundéré, P.O. Box 454, Ngaoundéré, Cameroon*
^{1,2,3}*ECS-Lab, EA3649, ENSEA, Cergy Cedex, Cergy-Pontoise 95014, France, Laboratoire QUARTZ EA 7393*

Abstract— The serial multicellular structure of static converters is widely used for high power applications. However, some controls of these converters are unreliable and are sensitive to fluctuations in some of its parameters. In this article is proposed a control by Petri nets that has overcome these deficiencies by making the converter robust vis-à-vis fluctuations that can affect the load or the input voltage. This has been successfully tested by digital simulation in the case of a two-cell converter connected to a non-strictly dissipative non-linear load.

Keywords— Petri nets control, robustness, multicellular converter, hybrid dynamic systems.

I. INTRODUCTION

The power electronics knows important technological developments. This is carried out thanks to the developments of the semiconductor of power components but also of new systems of energy conversion. Among these systems, multicellular converters are based on the association in series of the elementary cells of commutation. This structure appeared at the beginning of the 90's [1], makes it possible to share the constraints in tension and/or while running in high voltages installations by the cells of commutation series-connected and also to improve the harmonic contents of the forms of waves.

Several patents have been filed on this subject [2]. This new topology is becoming more and more attractive in industrial applications. Indeed, this multicellular structure is an interesting system for high power applications. To benefit as well as possible from the large potential of the multicellular structure, various studies have been developed in the literature. Further, the normal operation of the p-cell conversion series is obtained when the voltages are multiples of E/p , where E is the source voltage and p is the number of cells. This structure divides the voltage by distributing it over several cells in series, improves the spectral quality of the cut voltage and reduces the ripples of the voltage [3]. Several models, of this type of converter, are used for the development of open-loop [4] and closed-loop control laws [5]. Nevertheless, the current control algorithms do not take into account its hybrid character. In this article, our goal is to design and test a Petri nets control, based on an instantaneous model describing the hybrid behavior of the multicell converter.

After describing a model of the multicell converter in section 2, section 3 presents the Petri net control strategy. The implementation of the proposed control for simulation for the case of a two-cell converter connected to a non-strictly dissipative nonlinear load is described in section 4.

II. MULTICELLULAR CONVERTER MODEL

Throughout the paper, the p-cell converter connects in series p elementary cells and a passive load R and L as illustrated in figure 1. Each switching cell is controlled by a binary input signal $u_k(t)$ for $k = 1 \dots p$. This signal $u_k(t)$ is equal to 1 when the upper switch of the cell is conducting and 0 when the lower complementary switch of the cell is conducting. In order to ensure that, we must determine the floating capacitor voltages:

$$V_{cellk} = V_{C_k} - V_{C_{k-1}} = k \frac{E}{p}; \quad k = 1 \dots p \quad (1)$$

where $V_{C_0} = 0$; $V_{C_p} = E$,

From equation. (1), for $k = 1$, we have:

$$V_{cell1} = V_{C_1} - V_{C_0} = \frac{E}{p} \Rightarrow V_{C_1} = \frac{E}{p} \quad (2)$$

Increasing k , we find the general expression for the capacitor voltages:

$$V_{C_k} = k \frac{E}{p} \quad (3)$$

In order to determine the converter model, we consider two adjacent cells: $cell_k$ and $cell_{k+1}$ connected with the capacitor C_k (Figure 1). The capacitor voltage V_{C_k} is determined by the evolution of the capacitor current. This, in turn, is given by the configuration of the switches:

$$i_{C_k} = (u_{k+1} - u_k) i_L \quad (4)$$

Where $u_k = 1$ if the upper switch in $cell_k$ is conducting and $u_k = 0$ if the lower switch in $cell_k$ is conducting. The capacitor voltage is then given by equation (5):

$$i_{C_k} = C_k \frac{dV_{C_k}}{dt} \Rightarrow \frac{dV_{C_k}}{dt} = \frac{u_{k+1} - u_k}{C_k} \cdot i_L \quad (5)$$

Equation (5) can be generalized for all capacitors. Next we determine the output voltage as the sum of all cell voltages:

$$V_s = \sum_{k=1}^p V_{cell_k} = \sum_{k=1}^p (V_{C_k} - V_{C_{k-1}}) i_L \quad (6)$$

From equation (6), we note that we can have multiple voltage levels at the output, depending on the configuration of the switches. For a converter with p cells, we have $p + 1$ voltage levels: $0, \frac{E}{p}, \frac{2E}{p}, \dots, \frac{(p+1)E}{p}, E$. This means that the voltage jumps at the output are smaller than the ones in classical structures. For the multicell converter with an RL load in figure 1, the output current i_L is given by:

$$\frac{di_L}{dt} = \frac{V_s}{L} - \frac{R}{L} i_L \quad (7)$$

From equations (5), (6) and (7) we get the instantaneous model of the multicell converter in figure 2:

$$\begin{cases} \frac{di_L}{dt} = \frac{u_2 - u_1}{L} V_{C_1} + \frac{u_3 - u_2}{L} V_{C_2} + \dots \\ \quad + \frac{u_p - u_{p-1}}{L} V_{C_{p-1}} + \frac{u_p}{L} E - \frac{R}{L} i_L \\ \frac{dV_{C_1}}{dt} = \frac{u_2 - u_1}{C_1} i_L \\ \frac{dV_{C_2}}{dt} = \frac{u_3 - u_2}{C_2} i_L \\ \vdots \\ \frac{dV_{C_{p-1}}}{dt} = \frac{u_p - u_{p-1}}{C_{p-1}} i_L \end{cases} \quad (8)$$

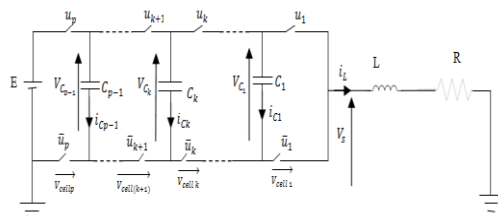


Figure 1: A p cells converter connected to RL load

where V_{C_k} is the k^{th} flying capacitor voltage and i_L is the output load current, which is the only measurable output. C_k for $k = 1 \dots p$; are the capacitors, E is the voltage of the source, R is the resistance and L is the inductance.

To simplify the study and the notations, we will study the overlapping operation of a converter with 2 cells (Figure 2). Its function is to supply a passive load (RL) in series with another nonlinear load connected in parallel with a capacitor [6]. Four operating modes are then possible as shown in figure 3. Note that the floating source takes part in the evolution of the dynamics of the system only to the third and fourth mode. In the third mode, the capacity discharges and charge during the fourth mode. Thus, if these two modes last same time with a constant charging current, then the average power transmitted by this floating source over one period of commutation is null. We also notice that these two modes make it possible to obtain by commutation the additional level $\frac{E}{2}$ on the output voltage V_s .

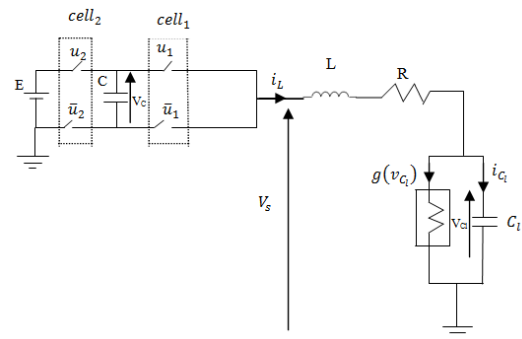


Figure 2: Two-cells chopper connected to a nonlinear load

As the switches of each cell are regarded as ideals, their behavior can be to model by a discrete state taking of the values 0 (*on*) or 1 (*off*). In practice, some of these states never will be visited for reasons of safety measures or following the strategy of order adopted or because of the structure of the converter him finally to even or comply with the rule of adjacency. The transitions are not necessarily controlled.

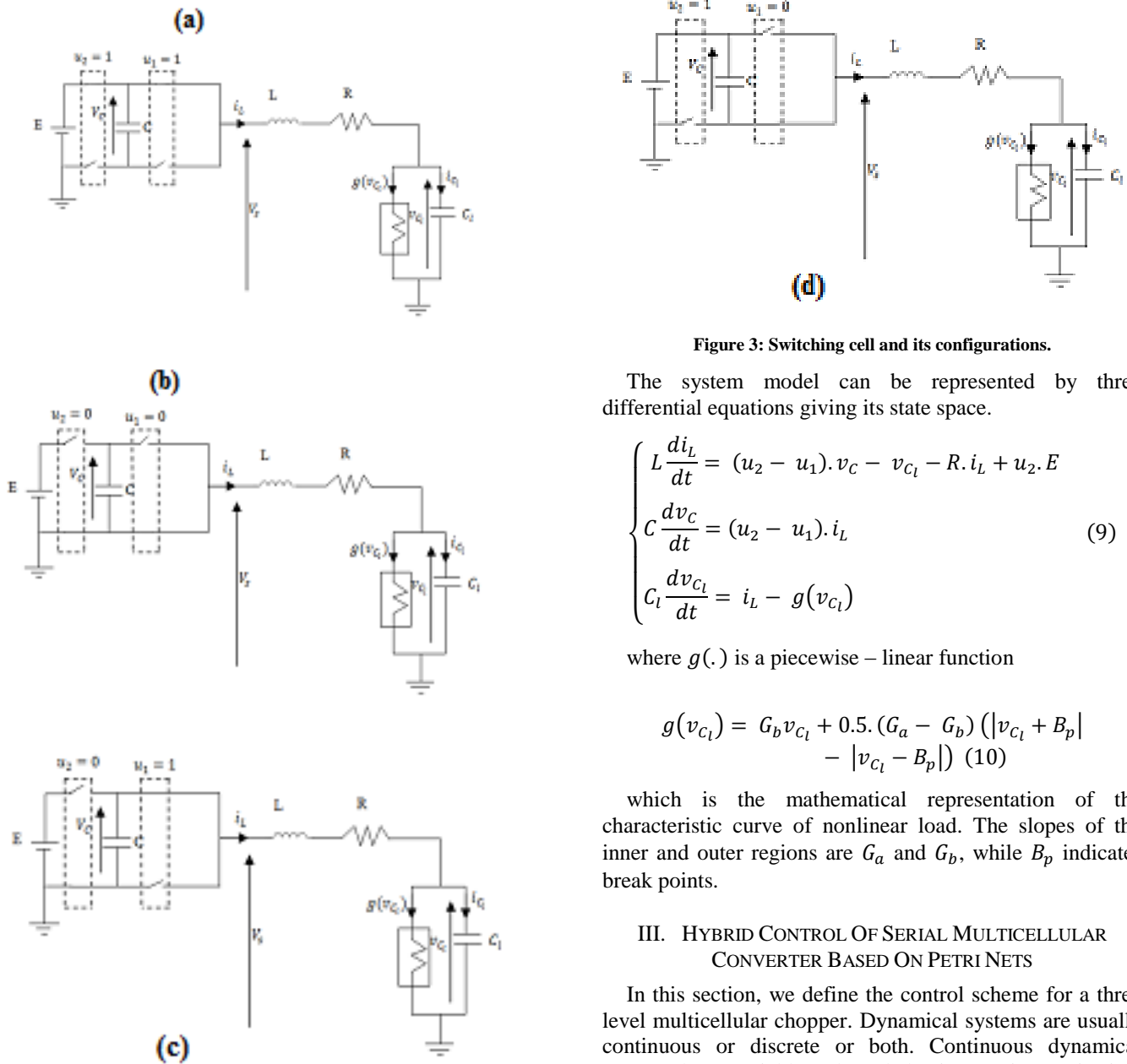


Figure 3: Switching cell and its configurations.

The system model can be represented by three differential equations giving its state space.

$$\begin{cases} L \frac{di_L}{dt} = (u_2 - u_1) \cdot v_C - v_{C1} - R \cdot i_L + u_2 \cdot E \\ C \frac{dv_C}{dt} = (u_2 - u_1) \cdot i_L \\ C_1 \frac{dv_{C1}}{dt} = i_L - g(v_{C1}) \end{cases} \quad (9)$$

where $g(\cdot)$ is a piecewise – linear function

$$g(v_{C1}) = G_b v_{C1} + 0.5 \cdot (G_a - G_b) (|v_{C1} + B_p| - |v_{C1} - B_p|) \quad (10)$$

which is the mathematical representation of the characteristic curve of nonlinear load. The slopes of the inner and outer regions are G_a and G_b , while B_p indicates break points.

III. HYBRID CONTROL OF SERIAL MULTICELLULAR CONVERTER BASED ON PETRI NETS

In this section, we define the control scheme for a three level multicellular chopper. Dynamical systems are usually continuous or discrete or both. Continuous dynamical systems have variables whose behavior continuous in time (voltage, current, speed, torque).

They are often modeled by differential equations or transfer functions. For discrete dynamical systems, the state space is a discrete set of Boolean value [7]. Systems including both continuous and discrete state are called hybrid dynamic systems (HDS). In a very simplified one HDS has two sub sets, a continuous block and a discrete block:

- ✓ The continuous block is the dynamic evolution of the state continues, in our case the RL connection.
- ✓ The block has the discrete system is discrete event receives internal events, external conditions

In this work, we were interested in modeling method and control systems hybrid event-based dominant the use of Petri nets [8]. The method is illustrated in Figure 4

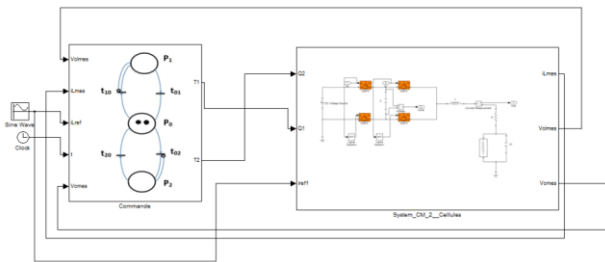


Figure 4: Global structure of the Petri net control

The control consists of two parts, a continuous and a discrete. The first is based on a classical PI control loop for regulating the output voltage. This loop has as input the error $E_1 = V_{cref} - V_C$ and I_{Lref} as output a current. The second control loop is done by a Petri net whose mission is the current regulation to value I_{Lref} calculated by the PI. The current regulation is followed by a voltage balancing to ensure a better distribution of the latter in each cell. For the current regulation, a hysteresis methodology is used. An operating band, $\pm\delta$, is provided, such that the output current, i_L , rests inside (i.e., $i_{Lref} - \delta \leq i_L \leq i_{Lref} + \delta$). Figure 5 represents the Petri net control of the switches, the places P_1 and P_2 respectively are modeling the state of the switches of cells $Cell_1$, and $Cell_2$. This algorithm is developed in order to control the system, in case it has an imbalance in the voltage of cells. The transition from one place to another is dependent on the voltage state (Table 2), current I_{Lref} and chopper configurations. The closure of the switch of the cell ($Cell_i$) depends on the validation of the transition t_{i0} and the elapsed delay d_i . This delay models the time allowed between two successive commutations, it is based on the technology used for making the switch. For our work we took the same delay ie $d = d_1 = d_2$.

In the Petri the role of two arcs inhibitors, is to prevent the presence of more than one, token in places P_1 and P_2 .

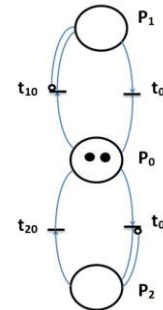


Figure 5: Petri net control switches of the converter

TABLE I:
Signification of places

Places P_i	Designations
P_0	Initial state
P_1	The switch of the first cell
P_2	The switch of the second cell

TABLE III:
The transitions

Transitions	Designations
t_{01}	$(e \geq +\delta)$ ou $((-\delta < e < +\delta)$ et $(V_C > E/2)$)
t_{02}	$(e \geq +\delta)$ ou $((-\delta < e < +\delta)$ et $(V_C < E/2)$)
t_{10}	$(e \leq -\delta)$ ou $((-\delta < e < +\delta)$ et $(V_C < E/2)$)
t_{20}	$(e \leq -\delta)$ ou $((-\delta < e < +\delta)$ et $(V_C > E/2)$)

The significance of all places and transition is shown in TABLE III and TABLE IV

IV. SIMULATIONS RESULTS

In this section the simulation results will be presented in order to show the behavior of the proposed control. The simulation parameters are the following:

- voltage source : $E = 100V$
- capacitances : $C = 0.1\mu F, C_1 = 40\mu F$
- $f_s = 20Hz$

- $L = 50mH$
- $R = 10\Omega$

Figure 6 and 7 respectively show the evolutions of the floating voltages V_C and the evolution of the current in the load i_L . We observe that the floating voltage reaches their reference and that the current in the load remains equal to the desired value i_{ch} . The error is greatly attenuated with a low rate of current ripple in the load, of the order of 0.5%. The major advantage of this command is its range of validity. Indeed, it has shown its effectiveness for different reference values i_{ref} . Figure 6 and 7 show that the proposed control strategy is effective and leads to satisfactory results and consistent objectives.

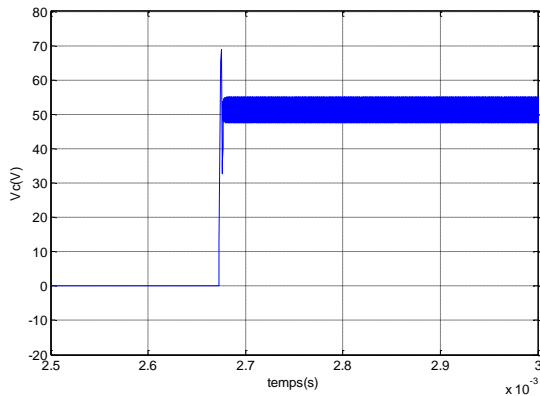


Figure 6 : Hybrid control based on Petri net

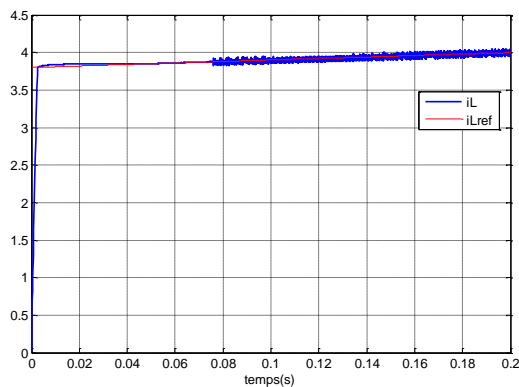


Figure 7: Hybrid control based on Petri net

V. CONCLUSION

In this paper a direct Petri nets control algorithm applied to a flying capacitor converter has been presented and developed. Petri nets are among the powerful tools for modeling and control of such systems which have discontinuities in their mathematical models. The proposed algorithm is based on the statements of floating capacitor, the current reference calculated by the PI and the authorized configurations. Finally simulation results show the convergence of the load current to a neighborhood of the value of the nominal operating current response times over. Furthermore an optimal steady-state trajectory is obtained according to the adjacency rules of the power switches. The simulation results affirm a good performance of the proposed Petri nets control.

REFERENCES

- [1] T. A. Meynard and H. Foch. Brevet français No. 91.09582 du 25 juillet 91, dépôt International PCT (Europe, Japon, USA, Canada) No. 92/00652 du 8 Juillet 92, 1991.
- [2] T. A. Meynard and H. Foch "Electronic device for electrical energy conversion between a voltage source and a current source by means of controllable switching cells", European Patent, 92/916336.8, 1992
- [3] S. Ben Said, K. Ben Saad and M. Benrejeb. "On a PI control of a multicellular converter". International Conference on Control, Engineering and Information Technology, 07-09 Juin Sousse 2013.
- [4] O. Tachon, M. Fadel and T. Meynard. "Control of series multicell converters by linear state feedback decoupling" EPF Grenoble, pp. 1588-1593, 1997.
- [5] O. Bethoux, J-P. Barbot. "Multi-cell chopper direct control law preserving optimal limit cycles". In IEEE CCA, 2002.
- [6] P. Djondiné, M. Ghanes, J-P. Barbot and B. Essimbi. "Dynamical behaviors of multicellular chopper". Journal of Control Science and Engineering, 2(1), 35-42, 2014
- [7] R. Goebel, J. Hespanha, A-R. Teel, C. Cai, and R. Sanfelice. "Hybrid systems: generalized solutions and robust stability". Proceedings of IFAC, Nolcos, 2004
- [8] S. Lafortune, G. Cassandra. "Introduction to discrete event systems" Published in september 1999 by Kuwer Academic Publishers, 848 pages. Hardbound
- [9] O. Bethoux, J. Barbot, "Commande permettant le contrôle du convertisseur multicellulaire série à nombre non premier de cellules". Revue science et technique de l'automatique. Vol 4, n°1 pp 44-49, 2007.
- [10] M. Fadel and T. A. Meynard. "Equilibrage des tensions dans les convertisseurs statiques multicellulaires série: Modélisation". EPF Grenoble, pp. 115-120, 1996.